Emissions of gas- and particle-phase polycyclic aromatic hydrocarbons (PAHs) in the Shing Mun Tunnel, Hong Kong

K.F. Ho [a,b], Steven Sai Hang Ho [a,c], S.C. Lee [a,*], Y. Cheng [b,d], Judith C. Chow [b,c], John G. Watson [b,c], P.K.K. Louie [e], Linwei Tian [f]

[a] Department of Civil and Structural Engineering, Research Center for Environmental Technology and Management, The Hong Kong Polytechnic University, Hung Hom, Kowloon, Hong Kong, China
[b] SKLLQG, Institute of Earth and Environment, CAS, Xi'an, Shaanxi 710075, China
[c] Division of Atmospheric Sciences, Desert Research Institute, 2215 Raggio Parkway, Reno, NV 89512, USA
[d] Department of Environmental Science and Technology, School of Human Settlements and Civil Engineering, Xi'an Jiaotong University, No.28 Xianning West Road, Xi'an, Shaanxi 710049, China
[e] Hong Kong Environmental Protection Department, 47/F, Revenue Tower, 5 Gloucester Road, Wan Chai, Hong Kong, China
[f] Department of Community and Family Medicine, School of Public Health, The Chinese University of Hong Kong, Hong Kong, China

ARTICLE INFO

ABSTRACT

Real-world vehicle emission factors for seventeen gas and particulate polycyclic aromatic hydrocarbons (PAHs) were quantified in the Shing Mun Tunnel, Hong Kong during summer and winter 2003. Naphthalene, acenaphthylene, and acenaphthene were the most abundant gas PAHs while fluoranthene and pyrene were the most abundant in the particle phase. Most (98%) of the gas PAHs consisted of two- and three-aromatic rings whereas most of the particle-phase PAHs were in four- ($\sim$60%) and five-ring ($\sim$17%) for fresh exhaust emissions. Average emission factors for the gas- and particle PAHs were 950–2564 μg veh^{-1} km^{-1} and 22–354 μg veh^{-1} km^{-1}, respectively. Good correlations were found between diesel markers (fluoranthene and pyrene; 0.85) and gasoline markers (benzo[ghi]perylene and indeno[1,2,3-cd]pyrene; 0.96). Higher PAH emission factors were associated with a higher fraction of diesel-fueled vehicles (DV) passing through the tunnel. Separate emission factors were determined from diesel and non-diesel exhaust by the regression intercept method. The average PAH emission factor (i.e., sum of gas and particle phases) from DV (3085 $\pm$ 1058 μg veh^{-1} km^{-1}) was $\sim$5 times higher than that from non-diesel-fueled vehicles (NDV, 566 $\pm$ 428 μg veh^{-1} km^{-1}). Ratios of DV to NDV emission factors were high for diesel markers ($>$24); and low for gasoline markers ($<$0.4).

© 2009 Elsevier Ltd. All rights reserved.

1. Introduction

Hong Kong, one of the most densely populated cities in the world, had 524,253 licensed vehicles in 2003 (Hong Kong Transport Department, 2006), with 23.6% as diesel-fueled. Gases and particulate matter (PM) emitted from mobile sources especially diesel-fueled vehicles (DV) have been associated with lung cancer and other non-cancer adverse respiratory diseases (IARC, 1983; Mauderly and Chow, 2008), visibility impairment (Watson, 2002), and climate change (MacCracken, 2008).

Chemical speciation of emission samples provides better understanding of pollution sources and their health and environmental impacts. Inorganic PM species (e.g., aluminum [Al], vanadium [V], and lead [Pb]) and extractable organic species (i.e., polycyclic aromatic hydrocarbons [PAHs], n-alkanes, carboxylic acids, and alkanols) have been used as markers of mobile source emissions for source apportionment (Ho et al., 2002; Lee et al., 2004; Wan et al., 2006; Tian et al., 2009). A few studies report the abundances of organic compounds in vehicle emissions as part of dynamometer, tunnels, and roadside studies (e.g., Chiang and Huang, 2009; Chow et al., 2007; Fraser et al., 1998; Fujita et al., 2007a,b; Marchand et al., 2004; Miguel et al., 1998; Olson and McDow, 2009; Watson et al., 2008). Vehicular emissions vary due to synthesis and application of different fuels, engine designs/maintenance, operation conditions, and types of emission controls (Turrio-Baldassarri et al., 2004).

PAHs are environmental pollutants known to be carcinogenic and mutagenic (IARC, 1983). They are important fractions of semi-volatile organic compounds (SVOCs); low molecular weight PAHs present as gases while high molecular weight PAHs are mainly associated with particles (Bidleman et al., 1986). Carcinogenic PAHs are mainly found

in the particle phase (Lyall et al., 1988). PAHs form from both natural and anthropogenic sources (i.e., incomplete combustion and pyrolysis of fossil fuels and other organic materials, Masclet et al., 1986), decompose under strong solar radiation (Baek et al., 1991a), undergo thermal decomposition, and react with other pollutants to produce more toxic derivative compounds (Nicolaou et al., 1984). Baek et al. (1991b) showed that vehicle emissions contribute to PAHs in urban and suburban areas, and other studies (Lee et al., 2001; Ho and Lee, 2002; Guo et al., 2003) confirmed that vehicular emissions are the most important source of PAHs in Hong Kong.

This study determines gas- and particle-phase PAH emission factors and emission profiles for vehicular emissions in Hong Kong. Samples were collected in a two-way heavily used tunnel and at roadside locations during winter and summer 2003. Seventeen PAHs, including 15 United States Environmental Protection Agency (U.S. EPA) priority PAHs (i.e., naphthalene, acenaphthylene, acenaphthene, fluorene, phenanthrene, anthracene, fluoranthene, pyrene, benzo[a]anthracene, chrysene, benzo[e]pyrene, benzo[b]fluoranthene, benzo[k]fluoranthene, benzo[a]pyrene, dibenzo[a,h]anthracene, benzo[ghi]perylene, and indeno[1,2,3-cd]pyrene), were acquired on one- or two-hour integrated quartz-fiber filters and polyurethane foams (U.S. EPA, 1997). A reliable monitoring program to determine the PAH emission factors was developed that measured concentration differences between the tunnel inlet and outlet, traffic rates, and tunnel ventilation fluxes during sampling periods.

2. Methodology

2.1. Sampling

The Shing Mun Tunnel is a two-bore tunnel (north and south bores), 2.6 km in length (divided into 1.0 and 1.6 km at the east and west sides, respectively), with a traffic volume of ~53,000 vehicles per day (Hong Kong Census and Statistical Department, 2004), that connects two urban areas (Shatin and Tsuen Wan) in Hong Kong. Each bore contains two traffic lanes. As shown in Fig. 1, two sampling stations were placed in the south bore at 686 m from the entrance and 350 m from the exit on the west side of the tunnel which has a -1% grade from entrance to exit. The vehicle speed limit is 80 km h^{-1} and vehicles should be in a hot-stabilized mode when passing the sampling stations. The cross-sectional area of the tunnel is 70.0 m^2, and the ventilation system was not in operation during the sampling periods. Average wind speed was measured using two sensors installed on the wall of the tunnel ~2 m above the sampling stations. Samples covered a wide range of vehicle types. One- or two-hour PAH samples were collected simultaneously at the inlet and outlet stations, using two medium-volume total suspended particulate polyurethane foam (PUF) samplers (Model GPS-1, Andersen Instruments, Smyrna, GA, USA). The sampler consisted of two stages. The first stage was a quartz-fiber filter for the collection of particulate PAHs. The second stage consisted of PUF in combination with adsorbent resin XAD-4 (PUF/XAD-4/PUF "sandwich" cartridge) that was placed downstream of the filter to collect gas PAHs. Blank quartz filters were preheated at 900 °C for over 3 h before use, returned immediately to the laboratory after sampling, and stored in a freezer (at 4 °C). PUF and XAD-4 resins (SKC Inc., Eighty Four, PA, USA) were pre-cleaned with acetone and dichloromethane, respectively, for 16 h in Soxhlet extractors (Sin et al., 2003). Cleaned PUF was air-dried for 2–4 h and wrapped with cleaned aluminum foil, while XAD-4 resin was purged with nitrogen to dryness and stored in amber bottles before use. The PAH sampler was calibrated using a manometer and top loading orifice plate. Sampling was conducted at a flow rate of 230 L min^{-1}. Samplers were fixed on the ground with sampling inlets ~1.5 m above ground level. Flow rates were
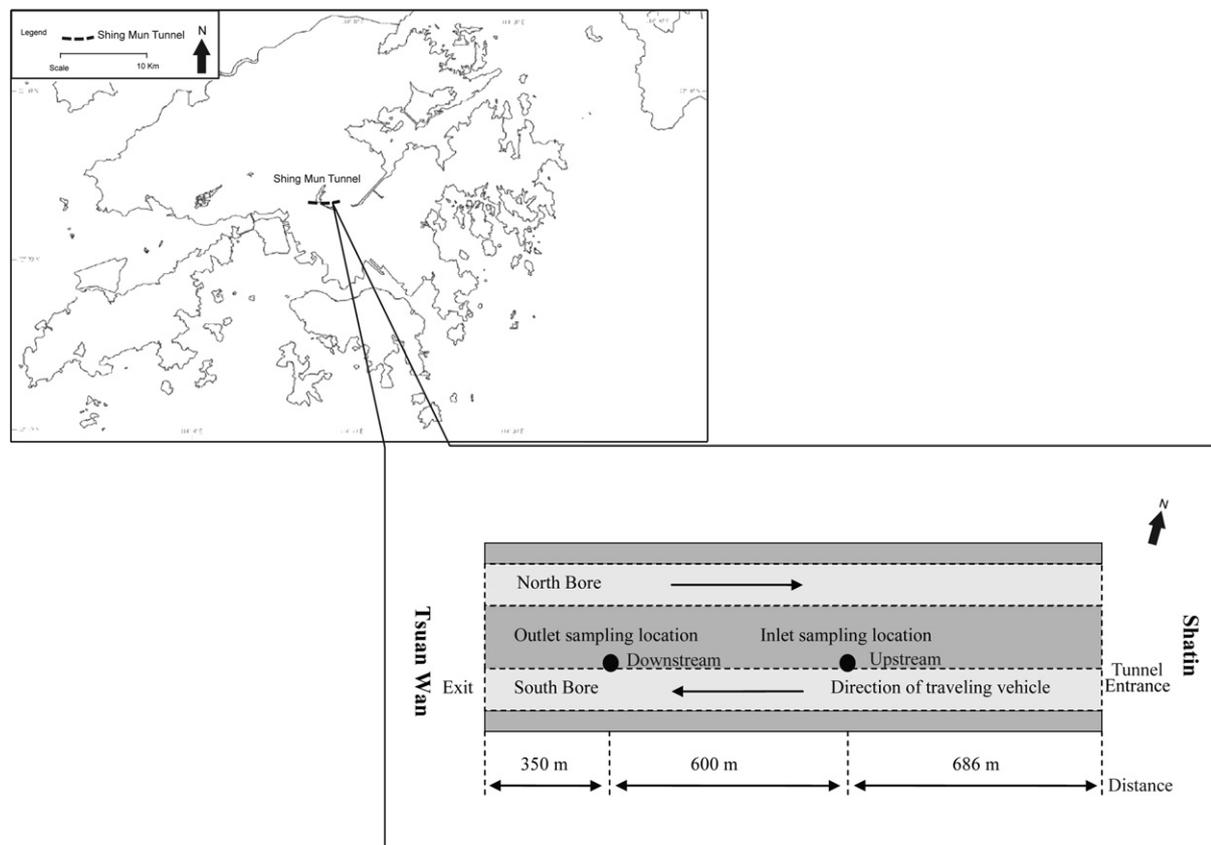

Fig. 1. Schematic diagram of the sampling configuration in the Shing Mun Tunnel, Hong Kong.

field-checked before and after each run using a calibrated flow meter. Vehicle fleet and traffic volume were determined during each sampling periods by manual counts at the tunnel entrance, along with video recording for data validation. Traffic counts reasonably agreed (standard deviation <10%) with Toll Plaza records collected ~200 m away from the tunnel entrance. Vehicles were classified into three major categories: 1) gasoline-fueled vehicles (e.g., motorcycles, private cars), 2) liquefied petroleum gas (LPG)-fueled taxis, and 3) diesel-fueled vehicles (e.g., large and mini-buses, light and heavy-duty trucks, light-duty trucks). Information on vehicle model years and odometer readings were not available in this study.

2.2. Chemical analysis

High purity solvents [high performance liquid chromatography (HPLC) grade or analytical reagent (AR) grade] were used for sample extraction. Each set of sampling media was extracted with 10% v/v diethyl ether in hexane for 16 h at 4 cycles per hour in a Soxhlet extractor, evaporated to dryness, reconstituted with cyclohexane, and concentrated in a Kuderna-Danish concentrator tube (Sin et al., 2003, 2005). The extract was cleaned up with a disposable silica gel column and eluted with 40% v/v dichloromethane in pentane. The eluent was evaporated and reconstituted with 1 mL acetonitrile. The concentrated sample extract was vortex-mixed and transferred to an amber glass vial for chromatographic analysis (Sin et al., 2003).

Samples were analyzed according to U.S. EPA Method TO-13 method (U.S. EPA, 1997) at the Hong Kong Government Lab. (HKGL). Twenty-five microliters of solution were injected into a gradient HPLC (Hewlett Packard 1100 system, Rockville, MD, USA) equipped with an ultraviolet (UV) and two fluorescence detectors (FL1 and FL2) connected in series for analysis. Samples were separated by a 4.6×250 mm Supelcosil LC-PAH C_{18} 5 µm reversed-phase analytical column (Bellefonte, PA, USA) at 27 ± 2 °C. The mobile phase consisted of two solvent mixtures: Mixture A-100% water (H_2O); and Mixture B-100% acetonitrile. The gradient program operated at 60% A/40% B mixture for 25 min, followed by a linear gradient to 100% mixture B for 20 min at a flow rate of 1.0 mL min^{-1}. The UV detector was set at the wavelength of 254 nm throughout the run. FL1 was set at the excitation wavelength (λ_{ex}) of 305 nm and the emission wavelength (λ_{em}) of 430 nm for the whole run. FL2 was programmed at 240 nm (λ_{ex}) and 425 nm (λ_{em}) for the first 28.5 min, and then changed to 300 nm (λ_{ex}) and 500 nm (λ_{em}) thereafter.

Target PAHs were identified and quantified using comparison of retention times and chromatographic peaks with those of known standards. Stock PAH standards were prepared by mixing pre-weighed chemicals (Accustandard, NH, USA) in acetonitrile and diluted into a range of 0.05–1.6 µg mL^{-1}. The National Institute of Standards and Technology (NIST; Gaithersburg, MD, USA) were used to verify the working standards. Five-point calibration plots achieved linear correlation coefficients $r^2 > 0.995$. Method detection limits (MDLs) are defined as 3.14 times the standard deviation of replicate analyses ($n \sim 7$) of blank PUF/XAD-4 resin spiked with a mixed standard of the lowest detectable concentrations (U.S. EPA, 1997). The MDL ranged from 0.5 to 4.3 ng sample among the 17 PAHs. The analytical protocol was validated by checking the spiked recovery of mid-point calibration mixed PAH standards on blank PUF and by performing replicate analyses of standard reference materials (i.e., NIST SRM 1647d) and urban dust (NIST SRM 1649a) for PAHs. The stability of the analytical system was monitored through plotting of control charts on the spike recovery of PAHs standards. The analytical uncertainty was within ±20%. Quality assurance/quality control (QA/QC) were periodically performed according to U.S. EPA Method TO-13 method (U.S. EPA, 1997).

Organic and elemental carbon were quantified by the IMPROVE thermal/optical reflectance protocol (Chow et al., 2004, 2007) on a DRI model 2001 carbon analyzer to determine the fraction of PAH in organic carbon.

2.3. Emission factor

Vehicle Emission factors from tunnel measurements were calculated according to Pierson and Brachaczek (1983) and Pierson et al. (1996). The emission factor is the mass of specific pollutant produced by a vehicle kilometer traveled (VKT), which can be determined using:

$$\text{EF}_{\text{veh}} = \frac{(C_{\text{out}} - C_{\text{in}})AUt}{NL} \tag{1}$$

where EF_{veh} is the average vehicular emission factor in µg veh^{-1} km^{-1} traveled, C_{out} and C_{in} represent the mass concentrations in µg m^{-3} of specific pollutants at the exit and entrance, respectively, A is the area of tunnel cross-section in m^2, U is the wind speed in m s^{-1}, t is the sample duration in h (1 or 2 h in this study), N is the number of passing vehicles during the sampling period, and L is the distance between the two monitoring stations in km (i.e., 0.6 km). This equation assumes that: 1) pollutants are long-lived species with negligible deposition, destruction, or reaction; and 2) movement of air and vehicles result in uniform mixing and pollutant distribution throughout the tunnel (El-Fadel and Hashisho, 2000). Eq. (1) was applied to each quantified PAH.

3. Results and discussion

3.1. PAH concentrations in the tunnel

Table 1 summarizes the measured PAH concentrations for different periods. Only six sample sets were acquired in the summer due to tunnel measurement restrictions. Gas-PAHs concentrations were 6–17 times higher than those of particle PAHs, with the exception of one sample set (on 25th August, 2003) collected during noon on a summer weekday (gas- to particle PAHs: 46); with the highest gas-PAHs concentration of 3664.7 ng m^{-3}. This sample corresponded with the highest diesel-vehicles counts (1821) and the highest ratio of diesel to gasoline vehicles (2.5) (see Table 1). This result is consistent with previous studies that diesel-vehicles emitted higher gas- and lower particle PAHs than gasoline vehicles (Westerholm et al., 1991; Hammerle et al., 1994; Westerholm and Egeback, 1994; Norbeck et al., 1998; Zielinska et al., 2004).

Naphthalene (352.4–810.8 ng m^{-3}), acenaphthylene (221.5–644.8 ng m^{-3}), and acenaphthene (620.5–1748.3 ng m^{-3}) are the most abundant gas PAHs, with two orders of magnitude lower concentrations in particle phases. Fluoranthene (20.0–42.4 ng m^{-3}) and pyrene (26.5–52.3 ng m^{-3}) are the most abundant particle-phase PAHs. Benzo[a]pyrene (BaP) is a probable human carcinogen and mainly present in the particle phase (Pankow, 1987; Wang et al., 2002). The average BaP (gas and particle phases) concentration was 5.9 ng m^{-3}, ranging from 1.3 to 11.9 ng m^{-3}. These values are 10 times higher than the average BaP of 0.49 ng m^{-3} determined at a Hong Kong roadside site (Lee et al., 2001; Ho and Lee, 2002). Large concentration variations were found for heavier PAHs in the particle phase (i.e., benzo[ghi]perylene and indeno[123-cd]pyrene), which ranged from below the detection limits to 20.8 ng m^{-3} and 0.15–11.4 ng m^{-3}, respectively.

Ratios of indeno[1,2,3-cd]pyrene to the sum of indeno[1,2,3-cd]pyrene and benzo[ghi]perylene (i.e., [I[cd]P/I[cd]P + B[ghi]P]) were 0.18 (gasoline), 0.37 (diesel), 0.56 (coal combustion), and 0.62 (wood burning) (Grimmer et al., 1983; Gogou et al., 1996). In Shing Mun Tunnel, these ratios ranged from 0.29 to 0.36, consistent with

Table 1
Average concentrations of gas, particle, and total PAHs for different time periods during the summer and winter of 2003 in the Shing Mun Tunnel, Hong Kong.

Polycyclic aromatic hydrocarbon (PAH) species	Concentrations (ng m^{-3})								
	Summer			Winter					
	Weekend		Weekday	Weekend		Weekday			
	Morning	Night	Noon	Morning	Night	Morning	Noon	Afternoon	Evening
1) Gas PAHs									
Naphthalene	403.4	482.6	791.2	764.0	471.6	810.8	572.7	352.4	509.1
Acenaphthylene	287.9	282.5	644.8	221.5	231.7	432.0	274.5	319.8	353.1
Acenaphthene	722.3	869.6	1748.3	620.5	706.7	1219.9	670.4	850.5	956.1
Fluorene	62.4	77.2	207.5	58.5	60.1	96.6	104.4	121.6	92.1
Phenanthrene	87.4	107.7	197.4	68.8	87.2	107.4	134.4	121.7	109.8
Anthracene	15.0	18.7	30.5	7.5	12.0	12.5	17.5	22.9	17.7
Fluoranthene	17.4	18.3	24.3	9.2	12.1	8.1	8.4	13.8	7.3
Pyrene	12.7	18.0	18.6	10.6	11.6	10.4	13.2	14.4	10.8
Benzo[a]anthracene	bd$^{\alpha}$	bd	0.03	bd	0.3	0.9	bd	0.4	bd
Chrysene	1.7	2.8	2.1	1.5	1.8	2.1	0.8	0.9	0.92
Benzo[e]pyrene	bd	bd	bd	0.29	0.47	1.2	bd	bd	0.23
Benzo[b]fluoranthene	bd	bd	bd	0.22	0.47	1.2	bd	bd	0.13
Benzo[k]fluoranthene	bd	bd	bd	0.07	0.17	0.61	bd	bd	0.09
Benzo[a]pyrene	bd	bd	bd	0.07	0.23	0.59	bd	bd	0.04
Dibenz[a,h]anthracene	bd	bd	bd	bd	bd	bd	bd	bd	bd
Benzo[ghi]perylene	bd	bd	bd	0.08	0.38	1.2	bd	bd	0.23
Indeno[1,2,3-cd]pyrene	bd	bd	bd	bd	bd	1.1	bd	bd	bd
Total Gas PAHs	1610.1	1877.5	3664.7	1762.8	1596.9	2703.6	1796.3	1818.4	2057.1
2) Particle PAHs									
Naphthalene	5.3	8.4	7.4	2.7	5.7	11.1	13.6	3.2	6.1
Acenaphthylene	bd	bd	bd	bd	bd	3.8	bd	0.81	bd
Acenaphthene	bd	bd	bd	bd	bd	6.4	bd	3.2	bd
Fluorene	0.63	0.6	1.4	1.0	1.1	1.7	1.1	1.1	0.80
Phenanthrene	7.8	7.0	7.9	3.1	8.6	14.1	5.8	10.3	6.3
Anthracene	1.4	1.2	1.3	1.8	2.8	3.0	1.9	2.7	2.0
Fluoranthene	28.1	42.4	20.7	27.8	39.5	34.7	20.0	24.4	24.0
Pyrene	34.7	52.3	26.5	35.7	49.6	44.1	28.6	32.1	34.2
Benzo[a]anthracene	15.2	20.8	5.2	11.4	20.3	9.0	4.8	6.8	7.2
Chrysene	19.2	23.9	6.0	19.6	31.2	15.8	8.8	10.1	11.8
Benzo[e]pyrene	4.6	15.2	bd	12.6	19.1	8.3	3.4	4.0	4.7
Benzo[b]fluoranthene	8.9	13.2	1.2	12.7	19.9	8.1	3.9	3.3	5.5
Benzo[k]fluoranthene	5.7	7.1	0.34	5.8	9.1	3.4	1.6	1.4	2.3
Benzo[a]pyrene	7.0	10.2	1.3	8.1	11.6	5.7	2.1	2.8	3.3
Dibenz[a,h]anthracene	0.18	0.51	0.30	bd	0.79	0.40	bd	0.22	0.09
Benzo[ghi]perylene	13.3	11.9	bd	12.4	20.8	11.1	6.0	7.2	7.5
Indeno[1,2,3-cd]pyrene	5.9	6.4	0.15	6.8	11.4	4.8	3.0	3.0	3.3
Total Particle PAHs	158.0	221.0	79.5	161.5	251.7	175.0	104.4	116.5	119.2
3) Gas + Particle PAHs									
Naphthalene	408.7	491.0	798.5	766.6	477.3	821.8	586.3	355.6	515.2
Acenaphthylene	287.9	282.5	644.8	221.5	231.7	435.7	274.5	320.6	353.1
Acenaphthene	722.3	869.6	1748.3	620.5	706.7	1226.3	670.4	853.7	956.1
Fluorene	63.0	77.8	208.9	59.5	61.3	98.3	105.5	122.7	92.9
Phenanthrene	95.1	114.7	205.3	71.9	95.9	121.5	140.2	132.0	116.1
Anthracene	16.3	19.9	31.8	9.3	14.9	15.5	19.3	25.5	19.7
Fluoranthene	45.5	60.6	45.0	37.1	51.6	42.9	28.3	38.2	31.4
Pyrene	47.4	70.3	45.2	46.3	61.3	54.4	41.8	46.5	45.0
Benzo[a]anthracene	15.2	20.8	5.2	11.4	20.6	9.8	4.8	7.2	7.2
Chrysene	20.9	26.8	8.0	21.1	33.0	17.9	9.6	11.0	12.8
Benzo[e]pyrene	4.6	15.2	bd	12.9	19.6	9.5	3.4	4.0	4.9
Benzo[b]fluoranthene	8.9	13.2	1.2	12.9	20.3	9.3	3.9	3.3	5.6
Benzo[k]fluoranthene	5.7	7.1	0.34	5.9	9.3	4.0	1.6	1.4	2.4
Benzo[a]pyrene	7.0	10.2	1.3	8.1	11.9	6.3	2.1	2.8	3.3
Dibenz[a,h]anthracene	0.18	0.51	0.30	bd	0.79	0.40	bd	0.22	0.09
Benzo[ghi]perylene	13.3	11.9	bd	12.5	21.1	12.3	6.0	7.2	7.8
Indeno[1,2,3-cd]pyrene	5.9	6.4	0.15	6.8	11.4	5.9	3.0	3.0	3.3
Total PAHs	1768.1	2098.5	3744.2	1924.3	1848.6	2892.0	1900.7	1935.0	2177.0
Number of samples	2	2	2	2	2	12	2	2	8
Average number of vehicles for each period									
Gasoline	802	1164	738	346	524	972	538	402	759
LPG	198	208	194	118	100	247	130	114	107
Diesel	692	646	1812	322	294	806	580	824	744
Total average number of vehicles	1692	2018	2744	786	918	2025	1248	1340	1610
Diesel/gasoline vehicle ratio	0.9	0.6	2.5	0.9	0.6	0.9	1.1	2.0	1.0
Diesel/non-diesel vehicle ratio	0.7	0.5	1.9	0.7	0.5	0.7	0.9	1.6	0.9

$^{\alpha}$bd denotes below method detection limits (MDLs).

abundant diesel vehicle emissions. Ratios of fluoranthene to the sum of fluoranthene and pyrene ([Flu/Flu + Pyr]) were consistent (0.41–0.45) in the Shing Mun Tunnel. The average ratio is the same as Sicre et al. (1987) reported for automobile emissions (0.43).

3.2. Distribution of PAHs in the gas and particle phases

Fig. 2 shows the distribution of PAHs in the gas and particle phases for summer and winter. The sum of two-ring (e.g., naphthalene) and three-ring (e.g., acenaphthylene, acenaphthene, fluorene, phenanthrene, and anthracene) PAHs accounted for ~98% of the total gas PAH concentrations, similar to findings of Westerholm et al. (1991), with abundant gas-phase three-ring PAHs. Less than 2% and <1% of gas-phase PAHs had four rings (e.g., fluoranthene, pyrene, benzo[a]anthracene, and chrysene, MW = 202–228) and five or six rings, respectively, due to their low vapor pressures. Conversely, two- and three-ring PAHs accounted for <9% of the particle PAHs, compared to ~60%, ~17%, and ~10% for four-, five-, and six-ring PAHs, respectively.
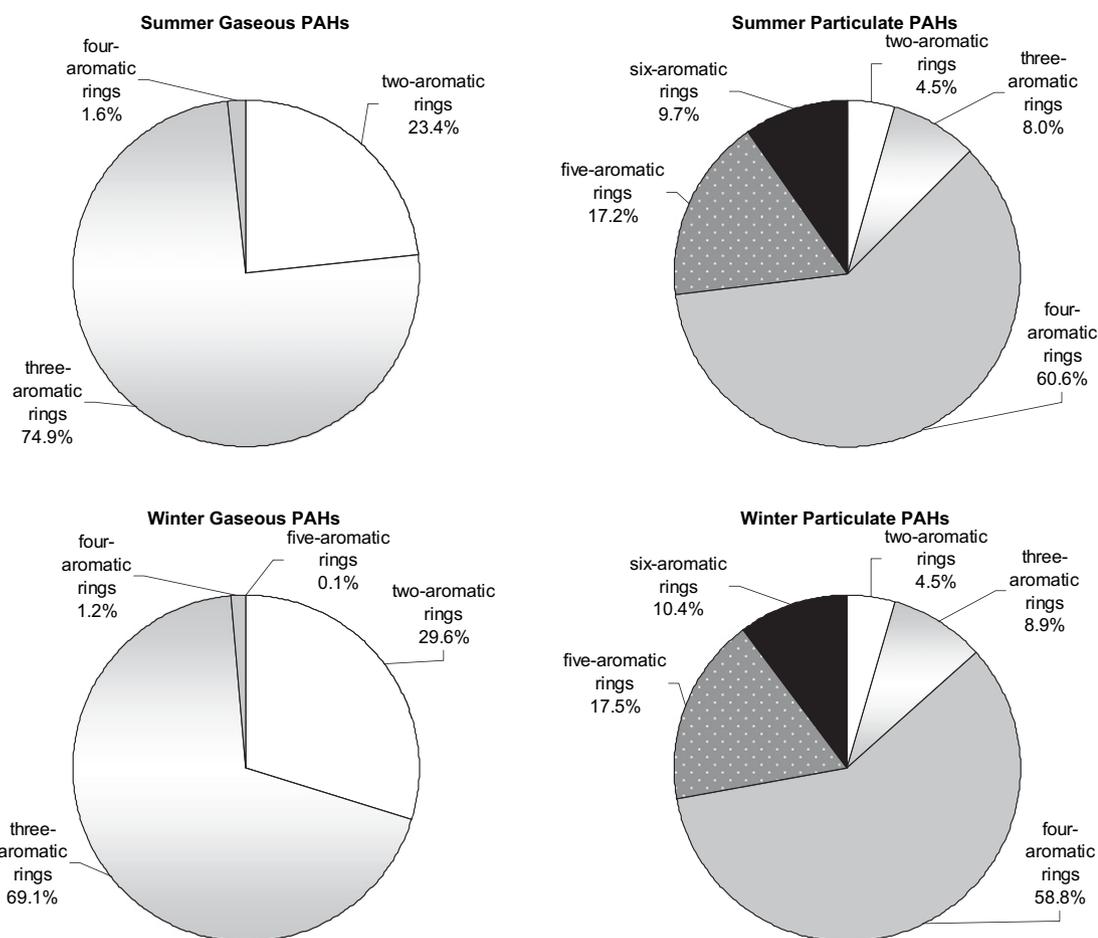
Similar gas/particle-phase distributions for individual PAHs were found between summer and winter, with a few exceptions shown in Fig. 3. For example, particulate anthracene increased from 8.5% to 13.6%, fluoranthene increased from 59.2% to 74.3%, and pyrene increased from 69.5% to 76.0% from summer to winter. Sin et al. (2003) found similar contrasts for ambient air samples in

Hong Kong. Lower temperatures in winter allow condensation of volatile and semi-volatile PAHs onto pre-existing particles.

3.3. Emission factors

Average emission factors for gas- and particle PAHs are shown in Table 2. Gas-PAHs emission factors ranged from 950 to 2563 µg per vehicle kilometer (µg veh^{-1} km^{-1}; average of 1551 ± 447 µg veh^{-1} km^{-1}). Particle-PAH emissions factors ranged from 22.0 to 354.2 µg veh^{-1} km^{-1} (average of 98 ± 80 µg veh^{-1} km^{-1}). Gas-PAHs emission factors were ~15 times higher than particle-PAHs emission factors. Emission factors for the five highest gas PAHs are: 1) acenaphthene, 2) naphthalene, 3) acenaphthylene, 4) phenanthrene, and 5) fluorene; and for the five highest particle PAHs are: 1) pyrene, 2) fluoranthene, 3) chrysene, 4) phenanthrene, and 5) naphthalene. Elevated particle emission factors were found for diesel and gasoline markers (e.g., fluoranthene, pyrene, benzo[ghi]perylene, and indeno[1,2,3-cd]pyrene), consistent with those reported in Ho et al. (2002) for vehicles dominated roadside samples in Hong Kong.

Correlations (r) among total PAH emission factors are shown in Table 3. The correlation coefficients (r) were 0.85 between fluoranthene and pyrene (diesel markers) and 0.96 between benzo[ghi]perylene and indeno[1,2,3-cd]pyrene (gasoline markers). In general, the correlations between the particle PAHs were higher than those for gas PAHs. The correlation between gas fluoranthene and pyrene was

Summer Gaseous PAHs

four-aromatic rings 1.6%
two-aromatic rings 23.4%
three-aromatic rings 74.9%

Summer Particulate PAHs

six-aromatic rings 9.7%
two-aromatic rings 4.5%
three-aromatic rings 8.0%
five-aromatic rings 17.2%
four-aromatic rings 60.6%

Winter Gaseous PAHs

four-aromatic rings 1.2%
five-aromatic rings 0.1%
two-aromatic rings 29.6%
three-aromatic rings 69.1%

Winter Particulate PAHs

six-aromatic rings 10.4%
two-aromatic rings 4.5%
three-aromatic rings 8.9%
five-aromatic rings 17.5%
four-aromatic rings 58.8%

Fig. 2. Gas and particle PAHs contributions, classified by the numbers of aromatic rings in the compounds, to the total PAH in summer and winter. (Two-aromatic rings PAHs include naphthalene; three-aromatic rings PAHs include acenaphthylene, acenaphthene, fluorene, phenanthrene, anthracene; four-aromatic rings PAHs include fluoranthene, pyrene, benzo[a]anthracene, chrysene; five-aromatic rings PAHs include benzo[e]pyrene, benzo[b]fluoranthene, benzo[k]fluoranthene, benzo[a]pyrene; and six-aromatic rings PAHs include dibenzo[a,h]anthracene, benzo[ghi]perylene, and indeno[1,2,3-cd]pyrene).
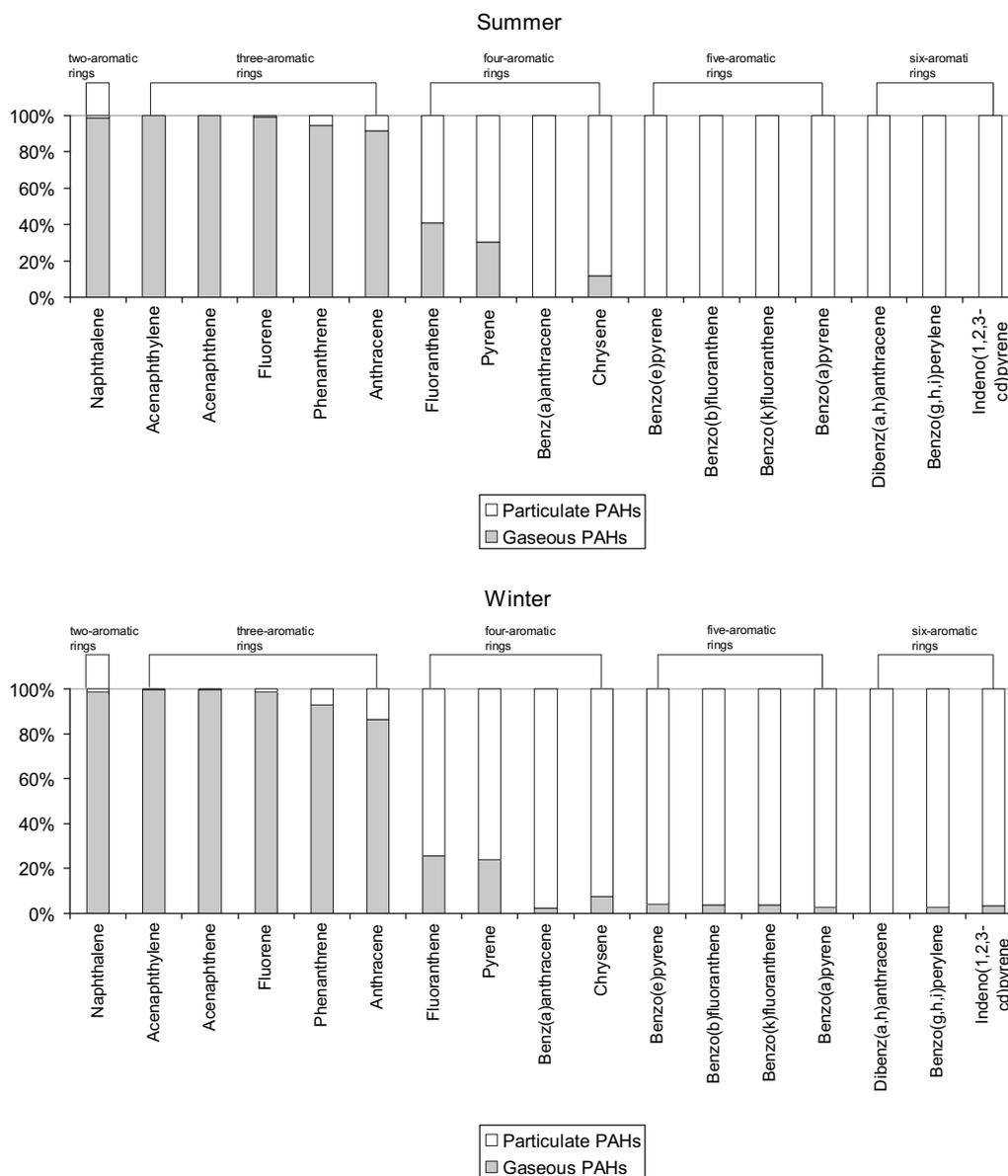
Summer

Winter

Fig. 3. Gas- and particle-phase distribution of individual PAHs in the Shing Mun tunnel during the summer and the winter testing period.

Table 2
Average PAHs emission factors measured in the Shing Mun Tunnel.

PAHs	No. of rings	MW (g)	Emission factor (μg veh^{-1} km^{-1})			Ratios of gas to particle PAHs
			Gas PAHs	Particle PAHs	Sum of PAHs	
Naphthalene	2	128	394.3 ± 135.2	8.5 ± 10.2	402.6 ± 136.2	46.4
Acenaphthylene	3	152	272.0 ± 88.8	0.2 ± 0.6	272.2 ± 89.0	1360.0
Acenaphthene	3	154	732.8 ± 254.0	0.6 ± 2.3	733.3 ± 254.4	1221.3
Fluorene	3	166	58.2 ± 19.2	1.3 ± 0.9	59.5 ± 19.8	44.8
Phenanthrene	3	178	67.5 ± 27.9	9.1 ± 6.2	76.6 ± 31.1	7.4
Anthracene	3	178	8.3 ± 5.7	1.9 ± 1.1	10.1 ± 6.4	4.4
Fluoranthene	4	202	7.3 ± 4.5	17.1 ± 10.0	24.4 ± 11.7	0.4
Pyrene	4	202	6.8 ± 3.9	23.5 ± 15.1	30.3 ± 16.4	0.3
Benzo[a]anthracene	4	228	0.3 ± 0.7	5.7 ± 5.7	5.9 ± 5.6	0.1
Chrysene	4	228	1.7 ± 1.5	10.4 ± 10.9	12.0 ± 11.6	0.2
Benzo[e]pyrene	5	252	0.6 ± 1.0	4.3 ± 7.1	4.9 ± 7.4	0.1
Benzo[b]fluoranthene	5	252	0.7 ± 1.0	5.4 ± 9.0	6.0 ± 9.3	0.1
Benzo[k]fluoranthene	5	252	0.3 ± 0.4	2.5 ± 4.2	2.8 ± 4.3	0.1
Benzo[a]pyrene	5	252	0.3 ± 0.5	2.3 ± 3.7	2.5 ± 3.9	0.1
Dibenzo[a,h]anthracene	5	278	0.0 ± 0.0	0.1 ± 0.2	0.1 ± 0.2	0.0
Benzo[ghi]perylene	6	276	0.4 ± 0.6	3.8 ± 6.5	4.2 ± 6.7	0.1
Indeno[1,2,3,cd]pyrene	6	276	0.1 ± 0.4	2.5 ± 4.1	2.6 ± 4.0	0.0
Total			1551.3 ± 447.4	98.2 ± 80.0	1649.4 ± 442.2	15.8

Table 3
Correlations coefficients (r) among emission factors for gas plus particle PAHs in the Shing Mun tunnel.

	1	2	3	4	5	6	7	8	9	10	11	12	13	14	15	16	17
Naphthalene (1)	1.00	0.57	0.74	0.34	0.31	0.25	−0.05	0.04	0.05	−0.09	−0.10	−0.06	−0.06	−0.08	−0.12	−0.07	−0.03
Acenaphthylene (2)		1.00	0.82	0.38	0.04	0.24	0.04	−0.24	−0.37	−0.26	−0.40	−0.40	−0.40	−0.34	−0.29	−0.39	−0.39
Acenaphthene (3)			1.00	0.25	−0.04	0.23	−0.26	−0.30	−0.29	−0.36	−0.42	−0.39	−0.37	−0.35	−0.15	−0.36	−0.36
Fluorene (4)				1.00	0.86	0.74	0.51	0.51	0.20	0.06	−0.02	−0.06	−0.09	−0.01	−0.12	−0.07	−0.03
Phenanthrene (5)					1.00	0.78	0.60	0.73	0.51	0.29	0.25	0.23	0.21	0.23	0.09	0.22	0.29
Anthracene (6)						1.00	0.29	0.40	0.24	−0.07	−0.22	−0.20	−0.19	−0.20	0.27	−0.11	−0.08
Fluoranthene (7)							1.00	0.85	0.65	0.79	0.62	0.60	0.57	0.61	0.00	0.59	0.60
Pyrene (8)								1.00	0.88	0.82	0.74	0.73	0.70	0.72	0.19	0.75	0.76
Benzo(a)anthracene (9)									1.00	0.86	0.83	0.86	0.85	0.82	0.37	0.89	0.92
Chrysene (10)										1.00	0.93	0.94	0.93	0.92	0.15	0.94	0.93
Benzo(e)pyrene (11)											1.00	0.99	0.98	0.99	0.08	0.93	0.96
Benzo(b)fluoranthene (12)												1.00	1.00	0.98	0.15	0.95	0.98
Benzo(k)fluoranthene (13)													1.00	0.97	0.14	0.94	0.98
Benzo(a)pyrene (14)														1.00	0.10	0.94	0.95
Dibenzo(a,h)anthracene (15)															1.00	0.34	0.25
Benzo(g,h,i)perylene (16)																1.00	0.96
Indeno(1,2,3-cd)pyrene (17)																	1.00

−0.28 compared to 0.97 in the particle phase, since those markers mostly in the particle phase, as shown in Fig. 3.

BaP has been used as a surrogate for total PAH (Minoia et al., 1997). A high correlation (r = 0.87) was found between the BaP and total particle PAH emission factors. However, Lee et al. (Lee et al., 2001) found that BaP may not be a preferred PAH surrogate in all cases due to its high reactivity and subject to reactivity losses during summer when solar radiation and ambient ozone levels are expected to reach the highest (Greenberg, 1989; DeWeist et al., 1981).

Table 4 compares PAHs emission factors with other tunnel studies. The total PAH emission factors (1649 µg veh^{-1} km^{-1}) in the Shing Mun Tunnel are >3 times higher than those in the Lundby Tunnel in Sweden (467 µg veh^{-1} km^{-1}) (Wingfors et al., 2001), which showed similar emission factors for BaP (2.5 and 2 µg veh^{-1} km^{-1}, respectively) in the two studies. Vehicle mix is different between the two tunnels with 8–24% diesel-fueled vehicles (DV) measured in the Lundby Tunnel as compared to ∼47% in the Shing Mun Tunnel. Emissions factors for fluoranthene (24 µg vel^{-1} km^{-1}) and pyrene

(30 µg vel^{-1} km^{-1}) in the Shing Mun Tunnel are closer to the values of 35 and 40 µg vel^{-1} km^{-1}, respectively reported in Tuscarora Mountain Tunnel in Pennsylvania, U.S., which is also influenced by heavy-duty vehicles (HEI, 2002). The measured emissions factor for phenanthrene (77 µg veh^{-1} km^{-1}) in the Shing Mun Tunnel was ∼2–4 times higher than the values found for a gasoline-fueled three-way catalytic converter (TWC) vehicle (28 µg vel^{-1} km^{-1}) and a heavy-duty diesel truck (40 µg vel^{-1} km^{-1}) (Boström et al., 2002). PAH contributions from asphalt and tires ware are included in these emissions.

3.4. Evaluation of gas and particle emissions from diesel-fueled vehicles

DV and non-DV emissions (NDV, including gasoline- and LPG-fueled vehicles) can be differentiated according to the method described by Pierson et al. (1996). The sample-specified emission factors were regressed against the fractions of DV and NDV, corresponding to each sample. For the nth sampling period, the EF$_n$

Table 4
Comparison of emission factors (µg veh^{-1} km^{-1}) for gas plus particle PAHs.

	This study	Benner et al., 1989	Wingfors et al., 2001	HEI, 2002	HEI, 2002
Tunnel, location	Shing Mun Tunnel, Hong Kong SAR	Baltimore Harbor Tunnel, MD, USA	Lundby Tunnel, Gothenburg, Sweden	Tuscarora Mountain Tunnel, Pennsylvania, USA[a]	Tuscarora Mountain Tunnel, Pennsylvania, USA[a]
Year of experiment	2003–2004	1993	1998	1999	1999
Type of vehicle	All	All	All	LD	HD
PAHs					
Naphthalene	402.6 ± 136.2	–	112	366.7 ± 893.5	2508.1 ± 6112.1
Acenaphthylene	272.2 ± 89.0	–	7.4	1.4 ± 234.5	339.1 ± 55,376.0
Acenaphthene	733.3 ± 254.4	–	6.9	11.4 ± 56.8	134.6 ± 669.4
Fluorene	59.5 ± 19.8	–	45	−3.6 ± 178.1	310.5 ± 15,266.5
Phenanthrene	76.6 ± 31.1	38 ± 13	166	−6.1 ± 75.1	448.3 ± 5540.2
Anthracene	10.1 ± 6.4	6 ± 3	12	12.8 ± 69.0	60.6 ± 325.5
Fluoranthene	24.4 ± 11.7	8 ± 3	51	1.6 ± 19.5	35.1 ± 423.9
Pyrene	30.3 ± 16.4	8 ± 3	60	−2.7 ± 21.4	40.7 ± 324.5
Benzo[a]anthracene	5.9 ± 5.6	2 ± 2	2.0	2.2 ± 5.0	1.2 ± 2.9
Chrysene	12.0 ± 11.6	3 ± 2	2.1	2.4 ± 7.2	0.7 ± 1.9
Benzo[e]pyrene	4.9 ± 7.4	1 ± 1	0.58	1.4 ± 3.8	0.4 ± 1.0
Benzo[b]fluoranthene	6.0 ± 9.3	–	0.67	–	–
Benzo[k]fluoranthene	2.8 ± 4.3	–	0.051	–	–
Benzo[a]pyrene	2.5 ± 3.9	2 ± 1	0.57	6.5 ± 13.7	6.2 ± 13.0
Dibenzo[a,h]anthracene	0.1 ± 0.2	–	0.095	–	–
Benzo[ghi]perylene	4.2 ± 6.7	2 ± 1	0.90	0.2 ± 4.2	2.9 ± 57.3
Indeno[1,2,3,cd]pyrene	2.6 ± 4.0	1 ± 1	0.26	0.9 ± 2.1	−0.1 ± 0.1
Total	1649.4	71	467.5	406.8	3887.9

Remarks: LD-Light Duty, HD-Heavy Duty.
[a] For species with near-zero emission rates and/or concentrations at or near the analytic detection limit, negative emission rates can result from this calculation.

Table 5
PAH emission factors for diesel-fueled vehicles (DV) and non-diesel-fueled vehicles (NDV) based on regression analysis of measurement acquired in the Shing Mun Tunnel.

PAHs	Emission factor (μg veh^{-1} km^{-1})		Correlation coefficient (r)	Ratio of DV/NDV
	DV	NDV[a]		
Naphthalene	613.4 ± 384.7	261.0 ± 155.6	0.26	2.35
Acenaphthylene	584.2 ± 209.6	46.3 ± 84.8	0.60	12.62
Acenaphthene	1479.1 ± 653.8	196.7 ± 264.4	0.50	7.52
Fluorene	105.3 ± 32.8	16.4 ± 12.9	0.65	6.42
Phenanthrene	153.2 ± 64.0	6.3 ± 26.2	0.60	24.32
Anthracene	22.5 ± 10.5	1.9 ± 4.2	0.56	11.84
Fluoranthene	50.7 ± 24.2	2.1 ± 9.9	0.55	24.14
Pyrene	60.5 ± 24.2	2.0 ± 9.9	0.62	30.00
Benzo[a]anthracene	10.8 ± 10.6	1.3 ± 4.4	0.28	8.31
Chrysene	18.3 ± 12.7	1.6 ± 5.2	0.37	11.43
Benzo[e]pyrene	4.4 ± 9.4	4.1 ± 3.7	0.01	1.07
Benzo[b]fluoranthene	0.7 ± 5.7	5.9 ± 2.3	−0.30	0.12
Benzo[k]fluoranthene	0.3 ± 2.4	2.4 ± 1.0	−0.31	0.13
Benzo[a]pyrene	2.9 ± 4.6	1.4 ± 1.8	0.11	2.07
Dibenzo[a,h]anthracene	0.4 ± 2.7	0.4 ± 1.2	−0.01	1.00
Benzo[ghi]perylene	1.1 ± 18.5	6.3 ± 7.4	−0.12	0.17
Indeno[1,2,3,cd]pyrene	1.0 ± 6.4	3.0 ± 2.5	−0.11	0.37
Total PAHs	3084.5 ± 1058.2	565.5 ± 427.9	0.57	5.45

[a] NDV: includes gasoline- and LPG-fueled vehicles.

is a weighed sum of the diesel emission factor, EF_{DV}, and the non-diesel emission factor, EF_{NDV}:

$$EF_n = x_n EF_{DV} + (1 - x_n)EF_{NDV} = x_n(EF_{DV} - EF_{NDV}) + EF_{NDV} \quad (2)$$

where x_n is the fraction of DV and $1 - x_n$ is the fraction of NDV corresponding to sample n. Extending the line derived to $x_n = 0$ and $x_n = 1$ provides EF_{DV} and EF_{NDV} estimates. Sampling periods were selected to obtain a wide range of DV fractions (Sagebiel et al., 1996). The standard error of the $x_n = 0$ intercept provides an estimate of the EF_{DV} and EF_{NDV} precisions. EF_{DV} and EF_{NDV} are assumed to be constant.

Table 5 summarizes the EF_{DV} and EF_{NDV} for each PAH. The EF_{DV} for total PAH (3085 ± 1058 μg veh^{-1} km^{-1}) was ~5 times higher than and the EF_{NDV} (566 ± 428 μg veh^{-1} km^{-1}). PAH emission factors are higher for the low MW, mostly gas-phase PAHs. The sum of naphthalene, acenaphthylene, acenaphthene, fluorene and phenanthrene accounted for ~95% of DV and 93% of NDV the total PAH emissions, respectively. High DV to NDV ratios (>24) were observed for diesel markers, phenanthrene, fluoranthene and pyrene; low DV/NDV ratios (<0.4) were found for gasoline markers, benzo[ghi]perylene and indeno[1,2,3-cd]pyrene. Measured PAHs typically comprise no more than 5% of the particulate organic carbon (OC), but their abundances are useful to distinguish DV and NDV emissions.

4. Conclusions

In Hong Kong during 2003, two- and three-ring PAHs (e.g., naphthalene, acenaphthylene, and acenaphthene) were the most abundant gas PAHs and four-ring PAHs (e.g., fluoranthene and pyrene) were the most abundant particle PAHs for hot-stabilized operation conditions. The average emission factor for gas PAHs (1551 ± 447 μg veh^{-1} km^{-1}) was >15 times higher than that for particle PAHs (98 ± 80 μg veh^{-1} km^{-1}). Good correlations were found for diesel- (e.g., fluoranthene and pyrene) and gasoline- (e.g., benzo[ghi]perylene and indeno[1,2,3-cd]pyrene) organic exhaust markers. Ratios of indeno[1,2,3-cd]pyrene to the sum of indeno[1,2,3-cd]pyrene and benzo[ghi]perylene evidence that diesel-fueled vehicle emission was dominant compared to that of gasoline and LPG in Hong Kong. Meanwhile, the total gas and particle PAH emission factor from diesel-fueled vehicles (3085 ± 1058 μg veh^{-1} km^{-1}) was ~5 times that from non-diesel vehicles (566 ± 428 μg veh^{-1} km^{-1}). Those results from this real-world study demonstrate that diesel-fueled vehicle emission is a large environmental concern in Hong Kong. Substitution of vehicle engines and application of environmental-friendly energy sources are possible solutions which can decrease the emissions of carcinogenic PAHs and improve the air quality.

References

Baek, S.O., Field, R.A., Goldstone, M.E., Kirk, P.W., Lester, J.N., Perry, R., 1991a. A review of atmospheric polycyclic aromatic hydrocarbons: source, fate and behavior. Water, Air and Soil Pollution 60, 279–300.

Baek, S.O., Goldstone, M.E., Kirk, P.W.W., Lester, J.N., Perry, R., 1991b. Phase distribution and particle size dependency of PAHs in urban atmosphere. Chemosphere 22, 503–520.

Benner, B.A., Gordon, G.E., Wise, S.A., 1989. Mobile sources of atmospheric polycyclic aromatic hydrocarbons: a roadway tunnel study. Environmental Science and Technology 23, 1269–1278.

Bidleman, T.F., Billings, W.N., Foreman, W.T., 1986. Vapor particle partitioning of semivolatile organic compounds – estimates from field collections. Environmental Science and Technology 20, 1038–1043.

Boström, C.-E., Gerde, P., Hanberg, A., Jernström, B., Johansson, C., Kyrklund, T., Rannug, A., Törnqvist, M., Westerholm, R., Victorin, K., 2002. Cancer risk assessment, indicators and guidelines for polycyclic aromatic hydrocarbons (PAH) in the ambient air. Environmental Health Perspectives 110 (Suppl. 3), 451–488.

Chiang, H.L., Huang, Y.S., 2009. Particulate matter emissions from on-road vehicles in a freeway tunnel study. Atmospheric Environment 43, 4014–4022.

Chow, J.C., Watson, J.G., Chen, L.W.A., Arnott, W.P., Moosmuller, H., 2004. Equivalence of elemental carbon by thermal/optical reflectance and transmittance with different temperature protocols. Environmental Science & Technology 38 (16), 4414–4422.

Chow, J.C., Watson, J.G., Lowenthal, D.H., Chen, L.W.A., Zielinska, B., Mazzoleni, L.R., Magliano, K.L., 2007. Evaluation of organic markers for chemical mass balance source apportionment at the Fresno Supersite. Atmospheric Chemistry and Physics 7, 1741–1754.

DeWeist, F., Golwinkler, R., Gielen, J., Rohdia, D., 1981. Influence of near ultraviolet irradiation on the mutagenicity of polycyclic aromatic hydrocarbons adsorbed on carbon black. In: Cooke, M., Dennis, A.J. (Eds.), Chemical Analysis and Biological Fate: Polynuclear Aromatic Hydrocarbons. Battelle Press, Columbus, OH, USA.

El-Fadel, M., Hashisho, Z., 2000. Vehicular emissions and air quality assessment in roadway tunnels: the Salim Slam tunnel. Transportation Research Part D: Transport and Environment 5, 355–372.

Fraser, M.P., Cass, G.R., Simoneit, B.R.T., 1998. Gas-phase and particle phase organic compounds emitted from motor vehicle traffics in a Los Angeles roadway tunnel. Environmental Science and Technology 32, 2051–2060.

Fujita, E.M., Campbell, D.E., Arnott, W.P., Chow, J.C., Zielinska, B., 2007a. Evaluations of the chemical mass balance method for determining contributions of gasoline and diesel exhaust to ambient carbonaceous aerosols. Journal of the Air & Waste Management Association 57, 721–740.

Fujita, E.M., Zielinska, B., Campbell, D.E., Arnott, W.P., Sagebiel, J.C., Mazzoleni, L.R., Chow, J.C., Gabele, P.A., Crews, W., Snow, R., Clark, N.N., Wayne, W.S., Lawson, D.R., 2007b. Variations in speciated emissions from spark-ignition and compression-ignition motor vehicles in California's south coast air basin. Journal of the Air & Waste Management Association 57, 705–720.

Gogou, A., Stratigakis, N., Kanakidou, M., Stephanou, E.G., 1996. Organic aerosols in Eastern Mediterranean: components source reconciliation by using molecular markers and atmospheric back trajectories. Organic Geochemistry 25, 79–96.

Greenberg, A., 1989. Phenomenological study of benzo[a]pyrene and cyclopenteno[cd]pyrene decay in ambient air using winter/summer comparisons. Atmospheric Environment 23, 2797–2799.

Grimmer, G., Jacob, J., Naujack, K.W., 1983. Profile of the polycyclic aromatic compounds from crude oils – inventory by GC GC–MS. PAH in environmental materials: Part 3. Fresenius Zeitschrift für Analytische Chemie 316, 29–36.

Guo, H., Lee, S.C., Ho, K.F., Wang, X.M., Zou, S.C., 2003. Particle-associated polycyclic aromatic hydrocarbons in urban air of Hong Kong. Atmospheric Environment 37, 5307–5317.

Hammerle, R., Schuetzle, D., Adams, W., 1994. A perspective on the potential development of environmentally acceptable light-duty diesel vehicles. Environmental Health Perspectives 102, 25–30.

Health Effects Institute, 2002. Emissions from Diesel and Gasoline Engines Measured in Highway Tunnels. Health Effects Institute, Boston MA.

Ho, K.F., Lee, S.C., Chiu, M.Y., 2002. Characterization of selected volatile organic compounds, polycyclic aromatic hydrocarbons and carbonyl compounds at a roadside monitoring station. Atmospheric Environment 36, 57–65.

Ho, K.F., Lee, S.C., 2002. Identification of atmospheric volatile organic compounds (VOCs), polycyclic aromatic hydrocarbons (PAHs) and carbonyl compounds in Hong Kong. Science of the Total Environment 289, 145–158.

Hong Kong Census and Statistical Department, 2004. Web site: http://www.censtatd.gov.hk/home/index.jsp.

Hong Kong Transport Department, December 2006, http://www.td.gov.hk/transport_in_hong_kong/transport_figures/index.htm.

International Agency for Research on Cancer (IARC), 1983. Monographs on the Evaluation of the Carcinogenic Risk of Chemicals to Humans: Polynuclear Aromatic Hydrocarbons, vol. 32. World Health Organization, Lyon, France.

Lee, S.C., Ho, K.F., Chan, L.Y., Zielinska, B., Chow, J.C., 2001. Polycyclic aromatic hydrocarbons (PAHs) and carbonyl compounds in urban atmosphere of Hong Kong. Atmospheric Environment 35, 5949–5960.

Lyall, R.J., Hooper, M.A., Mainwaring, S.J., 1988. Polycyclic aromatic hydrocarbons in the Latrobe Valley. Atmospheric Environment 22, 2549–2555.

MacCracken, M.C., 2008. Critical review: prospects for future climate change and the reasons for early action. Journal of the Air & Waste Management Association 58 (6), 735–786.

Marchand, N., Besombes, J.L., Chevron, N., Masclet, P., Aymoz, G., Jaffrezo, J.L., 2004. Polycyclic aromatic hydrocarbons (PAHs) in the atmospheres of two French alpine valleys: sources and temporal patterns. Atmospheric Chemistry and Physics 4, 1167–1181.

Masclet, P., Mouvier, G., Nikolaou, K., 1986. Relative decay index and sources of polycyclic aromatic hydrocarbons. Atmospheric Environment 20, 436–439.

Mauderly, J.L., Chow, J.C., 2008. Health effects of organic aerosols. Inhalation Toxicology 20, 257–288.

Miguel, A.H., Kirchstetter, T.W., Harley, R.A., 1998. On-road emissions of particulate polycyclic aromatic hydrocarbons and black carbon from gasoline and diesel vehicles. Environmental Science and Technology 32, 450–455.

Minoia, C., Magnaghi, S., Micoli, G., Fiorentino, M.L., Turci, R., Angeleri, S., Berri, A., 1997. Determination of environmental reference concentration of six PAHs in urban area (Pavia, Italy). Science of the Total Environment 198, 33–41.

Nicolaou, K., Masclet, P., Mouvier, G., 1984. Sources and chemical reactivity of polynuclear aromatic hydrocarbons in the atmosphere—a critical review. The Science of the Total Environment 32, 103–132.

Norbeck, J.M., Durbin, T.D., Truex, T.J., 1998. Final Report for Measurement of Primary Particulate Matter Emissions from Light-duty Motor Vehicles. CRC Project No. E-24-2; Submitted to Coordinating Research Council, Inc. and South Coast Air Quality Management District. Center for Environmental Research and Technology, University of California, Riverside, Riverside, CA.

Lee, J.H., Gigliotti, C.L., Offenberg, J.H., Eisenreich, S.J., Turpin, B.J., 2004. Sources of polycyclic aromatic hydrocarbons to the Hudson River Airshed. Atmospheric Environment 38, 5971–5981.

Olson, D.A., McDow, S.R., 2009. Near roadway concentrations of organic source markers. Atmospheric Environment 43, 2862–2867.

Pankow, J.F., 1987. Review and comparative analysis of the theories on partitioning between the gas and aerosol particulate phases in the atmosphere. Atmospheric Environment 21, 2275–2283.

Pierson, W.R., Brachaczek, W.W., 1983. Particulate matter associated with vehicles on the road. II. Aerosol Science and Technology 2, 1–20.

Pierson, W.R., Gertler, A.W., Robinson, N.F., Sagebiel, J.C., Zielinska, B., Bishop, G.A., Stedman, D.H., Zweidinger, R.B., Ray, W.D., 1996. Real-world automotive emissions: summary of studies in the Fort McHenry and Tuscarora mountain tunnels. Atmospheric Environment 30, 2233–2256.

Sagebiel, J.C., Zielinska, B., Pierson, W.R., Gertler, A.W., 1996. Real-world emissions and calculated reactivities of organic species from motor vehicles. Atmospheric Environment 30, 2287–2296.

Sicre, M.A., Marty, J.C., Saliot, S., Aparicio, X., Grimalt, J., Albaiges, J., 1987. Aliphatic and aromatic hydrocarbons in different sized aerosols over the Mediterranean Sea: occurrence and origin. Atmospheric Environment 21, 2247–2259.

Sin, D.W.M., Wong, Y.C., Choi, Y.Y., Lam, C.H., Louie, P.K.K., 2003. Distribution of polycyclic aromatic hydrocarbons in the atmosphere of Hong Kong. Journal of Environmental Monitoring 5, 989–996.

Sin, D.W.M., Fung, W.H., Choi, Y.Y., Lam, C.H., Louie, P.K.K., Chow, J.C., Watson, J.G., 2005. Seasonal and spatial variation of solvent extractable organic compounds in fine suspended particulate matter in Hong Kong. Journal of the Air & Waste Management Association 55, 291–301.

Tian, F., Chen, J., Qiao, X., Wang, Z., Yang, P., Wang, D., Ge, L., 2009. Sources and seasonal variation of atmospheric polycyclic aromatic hydrocarbons in Dalian, China: factor analysis with non-negative constraints combined with local source fingerprints. Atmospheric Environment 43, 2747–2753.

Turrio-Baldassarri, L., Battistelli, C.L., Conti, L., Crebelli, R., De Berardis, B., Iamiceli, A.L., Gambino, M., Iannaccone, S., 2004. Emission comparison of urban bus engine fueled with diesel oil and 'biodiesel' blend. Science of the Total Environment 327, 147–162.

United States Environmental Protection Agency (USEPA), 1997. Compendium of Methods for the Determination of Toxic Organic Compounds in Ambient Air. Method TO-13A: Determination of Polycyclic Aromatic Hydrocarbons (PAHs) in Ambient Air Using Gas Chromatography/mass Spectrometry (GC/MS). USEPA, Washington D.C.

Wan, Xianlie, Chen, Jingwen, Tian, Fulin, Sun, Weijun, Yang, Fenglin, Saiki, Kaoru, 2006. Source apportionment of PAHs in atmospheric particulates of Dalian: factor analysis with nonnegative constraints and emission inventory analysis. Atmospheric Environment 40, 6666–6675.

Wang, X.L., Tao, S., Xu, F.L., Dawson, R.W., Cao, J., Li, B.J., Fang, Y.J., 2002. Modeling the fate of benzo[a]pyrene in the waste water-irrigated areas of Tianjin with a fugacity mode. Journal of Environmental Quality 31, 896–903.

Watson, J.G., 2002. Visibility: science and regulation. Journal of Air & Waste Management Association 52 (6), 628–713.

Watson, J.G., Chen, L.W.A., Chow, J.C., Lowenthal, D.H., Doraiswamy, P., 2008. Source apportionment: findings from the U.S. Supersite program. Journal of the Air & Waste Management Association 58 (2), 265–288.

Westerholm, R., Egeback, K.E., 1994. Exhaust emissions from light- and heavy-duty vehicles: chemical composition, impact of exhaust after treatment, and fuel parameters. Environmental Health Perspectives 102, 12–23.

Westerholm, R.N., Almen, J., Li, H., Rannug, J.U., Egebaeck, K.E., Graegg, K., 1991. Chemical and biological characterization of particle-, semivolatile-, and gas-phase-associated compounds in diluted heavy-duty diesel exhausts: a comparison of three different semivolatile-phase samplers. Environmental Science and Technology 25, 332–338.

Wingfors, H., Sjödin, Å., Haglund, P., Brorström-Lundén, E., 2001. Characterization and determination of profiles of polycyclic aromatic hydrocarbons in a traffic tunnel in Gothenburg, Sweden. Atmospheric Environment 35, 6361–6369.

Zielinska, B., Sagebiel, J., Arnott, W.P., Rogers, C.F., Kelly, K.E., Wagner, D.A., Lighty, J.S., Sarofim, A.F., Palmer, G., 2004. Phase and size distribution of polycyclic aromatic hydrocarbons in diesel and gasoline vehicle emissions. Environmental Science and Technology 38, 2557–2567.